J|A|C|S
ARTICLES
Published on Web 02/22/2006

Structure and Multinuclear Solid-State NMR of a Highly Birefringent Lead−Gold Cyanide Coordination Polymer

Michael J. Katz,[†] Pedro M. Aguiar,[‡] Raymond J. Batchelor,[†] Alexei A. Bokov,[†] Zuo-Guang Ye,*[,†] Scott Kroeker,*[,‡] and Daniel B. Leznoff*[,†]

Contribution from the Department of Chemistry, Simon Fraser University, 8888 University Drive, Burnaby, BC, Canada V5A 1S6, and Department of Chemistry, University of Manitoba, Winnipeg, MB, Canada R3T 2N2

Received September 28, 2005; E-mail: dleznoff@sfu.ca; scott_kroeker@umanitoba.ca; zye@sfu.ca

Abstract: The coordination polymer $Pb(H_2O)[Au(CN)_2]_2$ (**1**) was synthesized by the reaction of $KAu(CN)_2$ and $Pb(NO_3)_2$. The structure contains 1-D chains of lead(II)−OH_2 linked via $Au(CN)_2^-$ moieties, generating a 2-D slab; weak aurophilic interactions of 3.506(2) and 3.4885(5) Å occur within and between slabs. The geometry about each lead(II) is bicapped trigonal prismatic, having six N-bound cyanides at the prism vertices and waters at two of the faces. Dehydration at 175 °C yields microcrystalline $Pb[Au(CN)_2]_2$ (**2**), which, along with **1**, was examined by ^{13}C, ^{15}N, ^{1}H, and ^{207}Pb solid-state NMR methods. Two ^{15}N resonances are assigned to the μ_2-bridging and hydrogen-bonding cyanides in **1**. Upon dehydration, the ^{207}Pb NMR spectrum becomes axially symmetric and yields a reduced shielding span, indicating higher site symmetry, while the ^{13}C and ^{15}N spectra reveal a single cyanide. Although no single-crystal X-ray structure of **2** could be obtained, a structure is proposed on the basis of the NMR and X-ray powder data, consisting of a lead(II) center in a distorted square-prismatic environment, with cyanides present at each corner. The birefringence of single crystals of **1** is found to be 7.0×10^{-2} at room temperature. This value is large compared to that of most optical materials and can be attributed to the anisotropy of the 2-D slabs of **1**, with all C≡N bonds aligned in the same direction by the polarizable lead(II) center.

Introduction

Research into the chemistry of supramolecular coordination polymers has rapidly grown in recent years due to an increasing demand for functional materials with conducting, magnetic, nonlinear optical, or zeolitic properties.[1] The modular nature of coordination polymer synthesis[2] allows the properties of each building block to be incorporated into the polymer. This concept has been used to great effect to target coordination polymers with interesting magnetic properties, in particular, by employing the very popular cyanometalate building blocks (e.g., Prussian blue-type systems).[3] In this light, it seems surprising that literature describing the incorporation of highly polarizable metal cations, such as lead(II), as building blocks in coordination polymers is unusually sparse,[4] despite the fact that such soft metal centers are key components in a range of nonlinear optical (NLO),[5] ferroelectric,[6] semiconductor,[7,8] and birefringent[9] materials. Indeed, the molecular coordination chemistry of lead(II) is well understood, featuring a vast number of binding modes and geometries ranging from three- to twelve-coordinate not often observed among transition metals.[10,11] As well, lead(II)

[†] Simon Fraser University.
[‡] University of Manitoba.

(1) (a) Janiak, C. *Dalton Trans.* **2003**, 2781. (b) Cassoux, P.; Valade, L.; Kobayashi, H.; Kobayashi, A.; Clark, R. A.; Underhill, A. E. *Coord. Chem. Rev.* **1991**, *110*, 115. (c) Ouahab, L. *J. Chem. Soc., Dalton Trans.* **1997**, *9*, 1909. (d) Decurtins, S.; Pellaux, R.; Antorrena, G.; Palacio, F. *Coord. Chem. Rev.* **1999**, *190−192*, 841. (e) Roundhill, D. M.; Fackler, J. P., Jr. *Optoelectronic Properties of Inorganic Compounds*; Plenum Press: New York, 1999.
(2) (a) Moler, D. B.; Li, H.; Chen, B.; Reineke, T. M.; O'Keeffe, M.; Yaghi, O. M. *Acc. Chem. Res.* **2001**, *34*, 319. (b) Chesnut, D. J.; Hagrman, D.; Zapf, P. J.; Hammond, R. P.; LaDuca, R.; Haushalter, R. C.; Zubieta, J. *Coord. Chem. Rev.* **1999**, *192*, 737.
(3) (a) Miller, J. S. *Inorg. Chem.* **2000**, *39*, 4392. (b) Verdaguer, M.; Bleuzen, A.; Marvaund, V.; Vaissermann, J.; Seuleiman, M.; Desplanches, C.; Scuiller, A.; Train, C.; Garde, R.; Gelly, G.; Lomenech, C.; Rosenman, I.; Veillet, P.; Cartier, C.; Villain, F. *Coord. Chem. Rev.* **1999**, *190*, 1023.
(4) For selected Pb(II) coordination polymers, see: (a) Yilmaz, V. T.; Caglar, S.; Harrison, W. T. A. *Z. Anorg. Allg. Chem.* **2004**, *630*, 948. (b) Foreman, M. R.; Plater, M. J.; Skakle, J. M. S. *J. Chem. Soc., Dalton Trans.* **2001**, 1897. (c) Zhu, L.-H.; Zeng, M.-H.; Ye, B.-H.; Chen, X.-M. *Z. Anorg. Allg. Chem.* **2004**, *630*, 952. (d) Li, G.; Hou, H.; Li, L.; Meng, X.; Fan, Y.; Zhu, Y. *Inorg. Chem.* **2003**, *42*, 4995. (e) Shi, Y.-J.; Li, L.-H.; Li, Y.-Z.; Chen, X.-T.; Xue, Z.; You, X.-Z. *Polyhedron* **2003**, *22*, 917.
(5) (a) Ye, Q.; Li, Y.-H.; Wu, Q.; Song, Y.-M.; Wang, J.-X.; Zhao, H.; Xiong, R.-G.; Xue, Z. *Chem.—Eur. J.* **2005**, *11*, 988. (b) Singh, N. B.; Suhre, D. R.; Green, K.; Fernelius, N.; Hopkins, F. K. *J. Cryst. Growth* **2005**, *274*, 132. (c) Sui, B.; Zhao, W.; Ma, G.; Okamura, T.-A.; Fan, J.; Li, Y.-Z.; Tang, S.-H.; Sun, W.-Y.; Ueyama, N. *J. Mater. Chem.* **2004**, *14*, 1631. (d) Meng, X.; Song, Y.; Hou, H.; Fan, Y.; Li, G.; Zhu, Y. *Inorg. Chem.* **2003**, *42*, 1306. (e) Guloy, A. M.; Tang, Z.; Miranda, P. B.; Srdanov, V. I. *Adv. Mater.* **2001**, *13*, 833. (f) Kondo, T.; Iwamoto, S.; Hayase, S.; Tanaka, K.; Ishi, J.; Mizuno, M.; Ema, K.; Ito, R. *Solid State Commun.* **1998**, *105*, 503.
(6) Newnham, R. *MRS Bull.* **1997**, *XXII*, 20.
(7) Kagan, C. R.; Mitzi, D. B.; Dimitrakopoulos, C. D. *Science* **1999**, *286*, 945.
(8) Mitzi, D. B.; Wang, S.; Feild, C. A.; Chess, C. A.; Guloy, A. M. *Science* **1995**, *267*, 1473.
(9) Sigman, M. B. J.; Korgel, B. A. *J. Am. Chem. Soc.* **2005**, *127*, 10089.
(10) (a) Holloway, C. E.; Melnik, M. *Main Group Metal Chemistry* **1997**, *20*, 399. (b) Parr, J. In *Comprehensive Coordination Chemistry II: From Biology to Nanotechnology*; Parkin, G. F. R., Ed.; Elsevier Pergamon: Boston, 2004; Vol. 3, p 545. (c) Engelhardt, L. M.; Patrick, J. M.; Whitaker, C. R.; White, A. H. *Aust. J. Chem.* **1987**, *40*, 2107. (d) Engelhardt, L. M.; Harrowfield, J. M.; Miyamae, H.; Patrick, J. M.; Skelton, B. W.; Soudi, A. A.; White, A. H. *Aust. J. Chem.* **1996**, *49*, 1111.
(11) Shimoni-Livny, L.; Glusker, J. P.; Bock, C. W. *Inorg. Chem.* **1998**, *37*, 1853.

compounds can have a stereochemically active lone pair of 6*s*-electrons, which, depending upon their degree of *p* character, can result in a more anisotropic geometry;[11] this effect can have a significant impact on the bulk properties of the material.

In addition to standard diffraction methods, lead-containing materials can be investigated by solid-state ^{207}Pb NMR. Lead-207 ($I = 1/2$, 22.1% natural abundance) NMR chemical shifts are extremely sensitive to small deviations in local structure. For example, solid $Pb(NO_3)_2$ is often used in solid-state NMR to calibrate probe temperature since its chemical shift changes by 0.70 ppm/K.[12,13] This sensitivity also manifests itself in very anisotropic chemical shieldings. Lead(II) compounds of higher point group symmetry exhibit shielding spans of 55−900 ppm, while those possessing lower symmetry tend to exhibit spans of 600−3800 ppm.[14−16] Although this can make it difficult to acquire ^{207}Pb NMR spectra of solids, it also makes such studies very attractive to characterize site symmetry.

The majority of reported lead(II)-based coordination polymers contain bridging halide ligands.[17] The $[(PbBr_2)_2(\mu\text{-pyrazine})]$ polymer contains 2-D Pb−Br sheets, which are distorted due to the stereochemical lone pair. The sheets are linked to one another via pyrazine ligand connectors.[17a] Such halide-bridged polymers, particularly those with iodide units, show a large third-harmonic NLO response with short response time (e.g., the layered polymer $(C_6H_{13}NH_3)_2PbI_4$).[5f] By incorporating a chiral organic fragment, large second-order NLO properties have been observed.[5e] Similar polymers containing tin(II) ions, which are less polarizable, yet still contain a potentially stereochemically active lone pair of electrons, have also been investigated.[7] These organic−inorganic hybrid materials show properties comparable to the best organic semiconductors made by vacuum evaporation, but allow a synthetically simpler route to highly ordered films. Conducting materials have also been synthesized with these tin(II) polymers by simply changing the organic portion of the polymer.[8]

Another common bridging unit is the family of cyanometalates $[M(CN)_x]^{n-}$, but within the vast cyanometalate coordination polymer literature,[18,19] the only lead-containing materials include organolead(IV) polymers with $[M(CN)_6]^{2-/3-}$ (M = Fe, Ru, Co) linkers,[20,21] a $Pb_2[Fe(CN)_6]$ semiconducting material whose structure was resolved only by powder X-ray diffraction,[22,23] and a lead(II) cyanoaurate system of undetermined structure exhibiting interesting luminescence behavior.[24] We have been investigating $Au(CN)_2$-based coordination polymers[25−28] in an effort to utilize the unique ability of d^{10}-metal centers, such as gold(I), to form attractive metallophilic bonds.[29−35] Motivated by our continuing interest in such polymers and the potentially useful properties accessible via the addition of a lead(II) building block, we have studied the aforementioned $Pb[Au(CN)_2]_2(H_2O)_x$ ($x = 0$, 1) system and hereby report its crystal structure, multinuclear solid-state NMR spectra, and high optical birefringence.

Experimental Section

General Procedures and Physical Measurements. All manipulations were performed in air. All reagents were obtained from commercial sources and used as received. Infrared spectra were recorded as KBr pressed pellets on a Thermo Nicolet Nexus 670 FT-IR spectrometer. Raman spectra were recorded on a Thermo Nicolet Nexus 670 FT-Raman spectrometer, equipped with a Nd:YAG laser (1064 nm). Microanalyses (C, H, N) were performed at Simon Fraser University by Mr. Miki Yang. Thermogravimetric analysis (TGA) data were collected using a Shimadzu TGA-50 instrument heating at 5 °C/min in an air atmosphere. Solid-state luminescence data were collected at room temperature on a Photon Technology International (PTI) fluorometer, using a Xe arc lamp, and a photomultiplier detector. X-ray powder patterns were collected on a Rigaku RAXIS rapid curved image plate area detector with graphite monochromator, utilizing Cu Kα radiation. One-hour scans were taken with a 0.3 μm collimator and a φ spinning speed of 5°/s; ω was held at 90°, and χ was held at 0°. The powder was adhered to a glass fiber with grease. Peak positions for **2** were located in WinPlotr.[36] Cell parameters were determined using Dicvol[37] and Treor.[38] Further refinement of the lattice parameters was performed using the FullProf package in WinPlotr.[36] Structural models for **2** were produced with Powder Cell[39] using triclinic symmetry. The final atomic positions were placed in a crystal data file and analyzed for existing symmetry elements using the MISSYM program,[40] thereby uniquely identifying the space group.

Solid-State NMR. ^{207}Pb, ^{1}H, ^{13}C, and ^{15}N NMR experiments were run on a Varian Inova 600 ($B_0 = 14.1$ T) at 195.08, 599.68, 150.79,

(12) van Gorkom, L. C. M.; Hook, J. M.; Logan, M. B.; Hanna, J. V.; Wasylishen, R. E. *Magn. Reson. Chem.* **1995**, *33*, 791.
(13) Bielecki, A.; Burum, D. P. *J. Magn. Reson. A* **1995**, *116*, 215.
(14) Nolle, A. *Z. Naturforsch.* **1977**, *32A*, 964.
(15) Sebald, A.; Harris, R. K. *Organometallics* **1990**, *9*, 2096.
(16) Fayon, F.; Farnan, I.; Bessada, C.; Coutures, J.; Massiot, D.; Coutures, J. P. *J. Am. Chem. Soc.* **1997**, *119*, 6837.
(17) (a) Shi, Y.-J.; Chen, X.-T.; Cai, C.-X.; Zhang, Y.; Xue, Z.; You, X.-Z.; Peng, S.-M.; Lee, G.-H. *Inorg. Chem. Commun.* **2002**, *5*, 621. (b) Shi, Y.-J.; Xu, Y.; Zhang, Y.; Huang, B.; Zhu, D.-R.; Jin, C.-M.; Zhu, H.-G.; Yu, Z.; Chen, X.-T.; You, X.-Z. *Chem. Lett.* **2001**, 678. (c) Calabrese, J.; Jones, N. L.; Harlow, R. L.; Herron, N.; Thorn, D. L.; Wang, Y. *J. Am. Chem. Soc.* **1991**, *113*, 2328. (d) Cui, Y.; Ren, J.; Chen, G.; Yu, W.; Qian, Y. *Acta Crystallogr. C* **2000**, *56*, e552. (e) Nordell, K. J.; Schultz, K. N.; Higgins, K. A.; Smith, M. D. *Polyhedron* **2004**, *23*, 2161. (f) Morsali, A.; Mahjoub, A. *Polyhedron* **2004**, *23*, 2427.
(18) Dunbar, K. R.; Heintz, R. A. *Prog. Inorg. Chem.* **1997**, *45*, 283.
(19) (a) Lefebvre, J.; Leznoff, D. B. In *Metal and Metalloid-Containing Polymers*; Wiley: New York, 2005; Vol. 5, pp 155−208. (b) Iwamoto, T. In *Comprehensive Supramolecular Chemistry*; Lehn, J. M., Atwood, J. L., Davies, J. E. D., MacNicol, D. D., Vögtle, F., Alberti, G., Bein, T., Eds.; Pergamon Press: Oxford, 1996. (c) Ohba, M.; Okawa, H. *Coord. Chem. Rev.* **2000**, *198*, 313.
(20) Brimah, A. K.; Schwarz, P.; Fischer, R. D.; Davies, N. A.; Harris, R. K. *J. Organomet. Chem.* **1998**, *568*, 1.
(21) Behrens, U.; Brimah, A. K.; Soliman, T. M.; Fischer, R. D.; Apperley, D. C.; Davies, N. A.; Harris, R. K. *Organometallics* **1992**, *11*, 1718.
(22) Zubkov, V. G.; Tyutyunnik, A. P.; Berger, I. F.; Maksimova, L. G.; Denisova, T. A.; Polyakov, E. V.; Kaplan, I. G.; Voronin, V. I. *Solid State Sci.* **2001**, *3*, 361.
(23) Zhukov, V. P.; Zainullina, V. M.; Zubkov, V. G.; Tyutyunnik, A. P.; Denisova, T. A. *Solid State Sci.* **2001**, *3*, 539.
(24) Patterson, H. H.; Bourassa, J.; Shankle, G. *Inorg. Chim. Acta* **1994**, *226*, 345.
(25) Leznoff, D. B.; Xue, B.-Y.; Patrick, B. O.; Sanchez, V.; Thompson, R. C. *Chem. Commun.* **2001**, *3*, 259.
(26) Leznoff, D. B.; Xue, B.-Y.; Stevens, C. L.; Storr, A.; Thompson, R. C.; Patrick, B. O. *Polyhedron* **2001**, *20*, 1247.
(27) Leznoff, D. B.; Xue, B.-Y.; Batchelor, R. J.; Einstein, F. W. B.; Patrick, B. O. *Inorg. Chem.* **2001**, *40*, 6026.
(28) Lefebvre, J.; Batchelor, R. J.; Leznoff, D. B. *J. Am. Chem. Soc.* **2004**, *126*, 16117.
(29) Rawashdeh-Omary, M. A.; Omary, M. A.; Patterson, H. H. *J. Am. Chem. Soc.* **2000**, *122*, 10371.
(30) Rawashdeh-Omary, M. A.; Omary, M. A.; Patterson, H. H.; Fackler, J. P., Jr. *J. Am. Chem. Soc.* **2001**, *123*, 11237.
(31) Fernandez, E. J.; Lopez-de-Luzuriaga, J. M.; Monge, M.; Olmos, M. E.; Perez, J.; Laguna, A. *J. Am. Chem. Soc.* **2002**, *124*, 5942.
(32) Fernandez, E. J.; Lopez-de-Luzuriaga, J. M.; Monge, M.; Olmos, M. E.; Perez, J.; Laguna, A.; Mohamed, A. A.; Fackler, J. P., Jr. *J. Am. Chem. Soc.* **2003**, *125*, 2022.
(33) Wang, S.; Garzon, G.; King, C.; Wang, J.-C.; Fackler, J. P., Jr. *Inorg. Chem.* **1989**, *28*, 4623.
(34) Bardají, M.; Laguna, A. *J. Chem. Educ.* **1999**, *76*, 201.
(35) Pyykkö, P. *Angew. Chem., Int. Ed.* **2004**, *43*, 4412.
(36) Roisnel, T.; Rodríguez-Carvajal, J. In *Materials Science Forum*, Proceedings of the Seventh European Powder Diffraction Conference (EPDIC 7); Delhez, R., Mittenmeijer, E. J., Eds.; 2000; p 118.
(37) Boultif, A.; Louër, D. *J. Appl. Crystallogr.* **1991**, *24*, 987.
(38) Werner, P.-E.; Eriksson, L.; Westdahl, M. *J. Appl. Crystallogr.* **1985**, *18*, 367.
(39) Kraus, W.; Nolze, G. *J. Appl. Crystallogr.* **1996**, *29*, 301.
(40) Gabe, E. J.; Page, Y. L.; Charland, J. P.; Lee, F. L.; White, P. S. *J. Appl. Crystallogr.* **1989**, *22*, 384.

and 60.77 MHz, respectively, using 3.2 and 5 mm double-resonance magic-angle spinning (MAS) probes.

A. Pb-207. A single-pulse experiment was employed for the MAS spectra with a 1 μs pulse (18° tip angle), using recycle delays of 5 and 10 s for **1** and **2**, respectively. Nonspinning experiments were acquired using a Hahn-echo, with pulse lengths of 5 and 10 μs and recycle delays of 10 and 25 s for **1** and **2**, respectively. Chemical shifts are reported with respect to $Pb(CH_3)_4$ using 1.0 M lead nitrate (−2961.2 ppm) as a secondary reference.[41]

To ensure that the measured chemical shifts are reliable, the effects of sample heating due to fast spinning were measured for spinning rates up to 11 kHz. The chemical shift was found to vary <0.1 ppm/K, as calibrated by $Pb(NO_3)_2$.[12,13] The small peak shift and symmetric line shape verify that the temperature dependence is too small to influence the data presented here.

B. H-1. Proton spectra were acquired using 1 μs pulse lengths (B_1 = 71.4 kHz), employing spinning speeds of 5 and 9 kHz and 20 s recycle delays. ^{1}H chemical shifts are relative to TMS, using water (+4.8 ppm) as a secondary reference.

C. C-13. $^{13}C\{^1H\}$ cross-polarization was employed for the MAS and nonspinning spectra of **1**, with recycle delays of 30 s. For **2**, a Bloch-decay sequence with 1 μs pulse (18° tip angle) and 60 s recycle delay was used. Nonspinning experiments were conducted with an echo pulse sequence to eliminate baseline distortions. ^{13}C chemical shifts are relative to TMS, using adamantane (29.5 and 38.6 ppm) as a secondary reference.

D. N-15. Spectra were acquired with single-pulse experiments using 2 μs pulse lengths (35° tip angle) and recycle delays of 720 s for **1**. Spectra of **2** were acquired with a 1 μs pulse length (18° tip angle) and a 120 s recycle delay. ^{15}N chemical shifts are relative to NH_3(l), using $^{15}NH_4{}^{15}NO_3$ (23.8 ppm, $^{15}NH_4$) as a secondary reference.

Birefringence. The birefringence was measured by means of polarized light microscopy utilizing an Olympus BX60 microscope, on plate-shaped single crystals of **1**. The optical retardation was measured using a tilting Berek compensator (3λ) at the wavelength of 546.1 nm. The birefringence was calculated by dividing the measured retardation by the crystal thickness of 26(2) μm. A heating/cooling stage (Linkam HTMS600) mounted on the microscope was used for studying the temperature dependence (150−340 K) of the birefringence.

Synthesis of $^{13}C^{15}N$-Enriched $K[Au(CN)_2]$. An aqueous solution of $K^{13}C^{15}N$/KCN (18 mg of $K^{13}C^{15}N$, 0.27 mmol; 41 mg of KCN, 0.63 mmol) was added to a suspension of AuCN (200 mg, 0.89 mmol) in 30 mL of water. The mixture was stirred and heated to 60 °C for 3 h, after which the remaining AuCN was filtered off. The water was removed in vacuo to yield a white precipitate of 15% $^{13}C^{15}N$-enriched $K[Au(CN)_2]$. Yield: 90 mg (35%). Anal. Calcd for C_2N_2AuK: C, 8.42%; H, 0.00%; N, 9.80%. Found: C, 8.11%; H, 0.00%; N, 9.47%. IR (KBr, cm^{-1}): 2152 (s), 2140 (s), 2101 (w), 2071 (s), 2063 (s).

$Pb(H_2O)[Au(CN)_2]_2$ (1). The addition of a 0.5 mL aqueous solution of $K[Au(CN)_2]$ (58 mg, 0.2 mmol) to a 0.5 mL aqueous solution of $Pb(NO_3)_2$ (33 mg, 0.1 mmol) generated an immediate pale yellow precipitate of $Pb(H_2O)[Au(CN)_2]_2$ (**1**), which was filtered and dried. Yield: 60 mg (83%). Anal. Calcd for $C_4H_2N_4Au_2OPb$: C, 6.64%; H, 0.28%; N, 7.75%. Found: C, 6.57%; H, 0.48%; N, 7.55%. IR (KBr, cm^{-1}): 3556 (w), 3476 (br), 2142 (s), 2131 (s), 1633 (w), 1593 (w). Raman (cm^{-1}): 2163 (s), 2153 (m).

Single crystals of **1** were synthesized as above, with both reactants dissolved in 10 mL of solvent. Slow evaporation yielded pale yellow crystals near dryness. The elemental analysis and IR spectra of the crystals were comparable with the powder.

Single crystals were also synthesized hydrothermally by heating the reactants to 125 °C, followed by slow cooling to room temperature over a three-day period.

(41) Maciel, G. E.; Dallas, J. L. *J. Am. Chem. Soc.* **1973**, *95*, 3039.

Table 1. Crystallographic Data for **1**

	1
empirical formula	$C_4H_2N_4Au_2OPb$
formula weight	723.22
crystal system	orthorhombic
space group	*Pcma*
a, Å	6.8938(8)
b, Å	9.8074(9)
c, Å	13.1773(19)
V, Å^3	890.92(18)
Z	4
T, K	293
λ, Å	0.70930
ρ_{calcd}, g·cm^{-3}	5.392
μ, mm^{-1}	51.725
R^a ($I > 2.5\sigma(I)$)	0.049
$R_w{}^a$ ($I > 2.5\sigma(I)$)	0.058
goodness of fit	1.25

[a] Function minimized $\sum w(|F_o| - |F_c|)^2$, where $w^{-1} = [\sigma^2(F_o) + (0.03*F_o)^2]$, $R = \sum||F_o| - |F_c||/\Sigma|F_o|$, $R_w = [\sum w(|F_o| - |F_c|)^2/\sum w|F_o|^2]^{1/2}$.

Isotopically Enriched 1. Reaction of 15% $^{13}C^{15}N$-enriched $K[Au(CN)_2]$ with $Pb(NO_3)_2$ as above generated a partially $^{13}C^{15}N$-labeled **1** for solid-state NMR analysis. Anal. Calcd for $C_4H_2N_4Au_2OPb$: C, 6.71%; H, 0.28%; N, 7.81%. Found: C, 6.65%; H, 0.29%; N, 7.64%. IR (KBr, cm^{-1}): 3469 (br), 2152 (s), 2140 (s), 2070 (s), 2062 (s), 1633 (br), 1591 (m), 1386 (m).

$Pb[Au(CN)_2]_2$ (2). Solid **1** (60 mg, 0.083 mmol) was heated at 175 °C for 18 h, forming a powder of **2**. Yield: 59 mg (100%). Anal. Calcd for $C_4N_4Au_2Pb$: C, 6.81%; H, 0.00%; N, 7.94%. Found: C, 6.70%; H, 0.00%; N, 7.66%. IR (KBr, cm^{-1}): 2130 (s), 1631 (br), 1385 (m). Raman (cm^{-1}): 2154.

Isotopically Enriched 2. Labeled **2** was synthesized by heating labeled **1** at 175° for 18 h.

X-ray Crystallographic Analysis of $Pb(H_2O)[Au(CN)_2]_2$ (1). Crystallographic data for **1** are tabulated in Table 1. A pale yellow crystal of **1** having dimensions of 0.18 × 0.17 × 0.05 mm^3 was glued onto a glass fiber. The data range 4° ≤ 2θ ≤ 62° was recorded with the diffractometer control program DIFRAC[42] and an Enraf Nonius CAD4F diffractometer with Mo Kα radiation. The data were corrected by integration for the effects of absorption with a transmission range of 0.073−0.162. Data reduction included corrections for Lorentz and polarization effects. Final unit-cell dimensions were determined on the basis of 53 well-centered reflections with range 40° ≤ 2θ ≤ 45°.

The programs used for the absorption correction and data reduction were from the NRCVAX Crystal Structure System.[40] The structure was solved and refined using CRYSTALS.[43] Diagrams were made using ORTEP-3[44] and POV-RAY.[45] Complex scattering factors for neutral atoms were used in the calculation of structure factors.[46]

The coordinates and anisotropic displacement parameters for the non-hydrogen atoms of **1** were refined. Hydrogen atoms were placed in geometrically calculated positions and refined using a riding model and a constrained isotropic thermal parameter. The final refinement using observed data ($I_o \geq 2.50\sigma(I_o)$) and statistical weights included 75 parameters for 805 unique reflections. Selected bond lengths and angles are given in Table 2.

The structure of **1** appears to exhibit some disorder, which is partially modeled by 4% occupancy alternate sites for the lead and gold atoms

(42) Gabe, E. J.; White, P. S.; Enright, G. D. *DIFRAC: A Fortran 77 Control Routine for 4-Circle Diffractometers*; N. R. C.: Ottawa, 1995.
(43) Betteridge, P. W.; Carruthers, J. R.; Cooper, R. I.; Prout, K.; Watkin, D. J. *J. Appl. Crystallogr.* **2003**, *36*, 1487.
(44) Farrugia, L. J. *J. Appl. Crystallogr.* **1997**, *30*, 565.
(45) Fenn, T. D.; Ringe, D.; Petsko, G. A. *J. Appl. Crystallogr.* **2003**, *36*, 944 (Persistence of Vision Raytracing: http://www.povray.org).
(46) *International Tables for X-ray Crystallography*; Kynoch Press: Birmingham, U.K. (present distributor Kluwer Academic Publishers: Boston, MA), 1975; Vol. IV.

Table 2. Selected Bond Lengths (Å) and Angles (°) for **1**[a]

Pb(1)−N(1)	2.595(18)	Pb(1)−N(2)	2.65(2)
Pb(1)−N(1′)	2.595(18)	Pb(1)−N(2′)	2.65(2)
Pb(1)−N(1*)	2.87(2)	Pb(1)−O(1)	2.57(2)
Pb(1)−O(1*)	2.83(2)	Au(1)−Au(2)	3.541(2)
Au(1)−Au(1″)	3.5222(8)	Au(2)−Au(1″)	3.454(2)
Pb(1)−N(1)−C(1)	138(2)	Pb(1)−N(2)−C(2)	132.1(19)
Pb(1)−N(1″)−C(1″)	125(2)	N(1)−Pb(1)−N(2)	83.1(6)
N(1)−Pb(1)−N(1″)	79.2(4)	N(1)−Pb(1)−N(1′)	87.2(9)
N(1)−Pb(1)−N(2′)	143.0(7)	N(1)−Pb(1)−N(1*)	132.4(3)
N(2)−Pb(1)−N(1″)	131.9(6)	N(2)−Pb(1)−N(2′)	83.5(8)
N(2)−Pb(1)−N(1*)	80.6(6)	N(1*)−Pb(1)−N(1″)	77.2(7)
O(1)−Pb(1)−O(1*)	122.7(7)		

[a] Symmetry transformations: ′, $x, -y-1, -z$; *, $x-1/2, -y+1, -z+1/2$; ″, $x-1/2, y, -z+1/2$.

only. The alternate (4%) sites for the cyanide and water groups were not modeled due to the very low electron density expected for these sites.

Results and Discussion

Structure of $Pb(H_2O)[Au(CN)_2]_2$ (1). The addition of 2 equiv of $K[Au(CN)_2]$ to a concentrated aqueous solution of $Pb(NO_3)_2$ resulted in the precipitation of the microcrystalline coordination polymer $Pb(H_2O)[Au(CN)_2]_2$ (**1**). The IR spectrum of **1** reveals two cyanide bands at 2140 and 2130 cm^{-1}, both of which are lower than the ν_{CN} of 2141 cm^{-1} for $K[Au(CN)_2]$, indicating bridging to another metal. Although ν_{CN} bands in most cyanometalates blue-shift upon nitrile binding,[18,47] the red-shift in **1** can be attributed to substantial back-bonding from the lead(II) center. The Raman spectrum also shows two ν_{CN} peaks at 2163 and 2153 cm^{-1}. The room temperature luminescence of **1** shows emission and excitation maxima at 520 and 420 nm, respectively, as previously reported by Patterson.[24]

The structure of **1** contains a Pb(II) center in a bicapped trigonal prism coordination geometry, defined by six cyanide nitrogens forming the vertices of the prism and two capping water molecules (Figure 1a). The water molecules bridge neighboring lead centers to form 1-D chains which are aligned down the 2-fold screw along the *a*-axis. The 1-D chains link to one another via $Au(CN)_2^-$ units, generating a 2-D slab of edge-sharing trigonal prismatic columns (Figure 1b). Weak aurophilic interactions of 3.506(2) Å occur within each slab (Figure 1, dashed lines). These slabs stack upon each other via hydrogen bonding (O(1)−N(2) 2.86(3) Å) and aurophilic interactions (Au(1)−Au(2) 3.488(5) Å). The layer of gold atoms shows a nearly close-packed environment. The $Au(CN)_2^-$ groups are nearly eclipsed, with a dihedral angle of <1°.[30,48] Selected bond lengths and angles can be found in Table 2.

Slight (4%) disorder in the structure was observed and appears to arise from an alternate choice of trigonal prismatic interstices, in which the 1-D chain of $Pb-OH_2$ is shifted by half a cell in the *a*-direction, effectively switching the location of the lead and water; this forces the gold atoms to reorganize slightly to accommodate the shifted chain.

Consistent with the IR data, there are two distinct cyanide units in the structure: CN(1) bridges two lead centers (μ_2-nitrile), while CN(2) binds only to one lead atom. A similar situation was observed in $Pb(dca)_2$ (dca = dicyanamide).[49,50] The CN(2) nitrile also accepts a hydrogen bond from a water molecule of the adjacent slab.

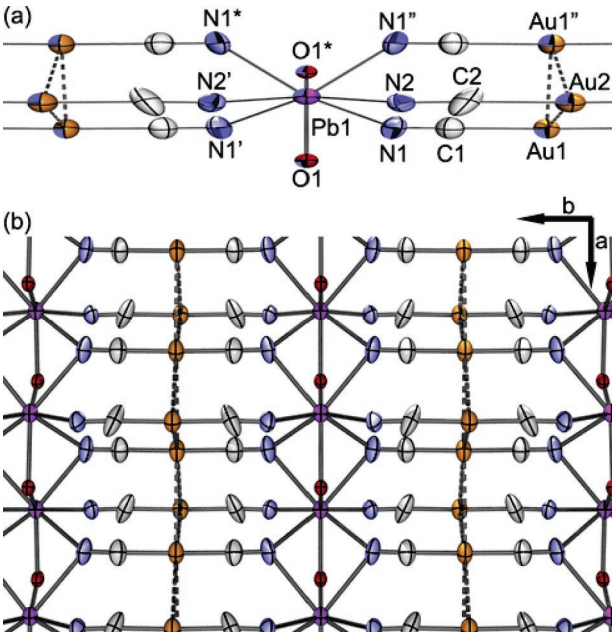

Figure 1. (a) Local site geometry about the Pb(II) center of **1**. (b) Two-dimensional slab of **1** viewed down the *c*-axis.

The eight-coordinate lead center shows an asymmetry in the bond lengths toward one hemisphere, which has been attributed to the presence of a stereochemically active lone pair on the lead(II), producing a hemi-directional structure (Table 2).[11,51] This asymmetry is exemplified by Pb(1)−N(1) and Pb(1)−N(1*) bond lengths of 2.62(3) and 2.87(3) Å, respectively; these are similar to $Pb(dca)_2$, which has Pb−N bond lengths of 2.679(6) and 2.868(10) Å.[49,50] The $Pb(1)-OH_2$ bonds also show an asymmetry associated with the lone pair's presence, with Pb(1)−O(1) and Pb(1)−O(1*) distances of 2.57(2) and 2.83(2) Å, respectively; these lengths are comparable to that of other water-bound lead complexes.[52]

In fact, there are relatively few compounds in which there are two H_2O units bound to a single lead(II) center; this paucity has generally been attributed to the low aqueous solubility of lead compounds.[11] The TGA of **1** demonstrates the loss of bound water over the broad temperature range of 100−200 °C, suggesting relatively strong H_2O binding to the lead center. The dehydrated structure is then stable up to 300 °C, at which point it decomposes via loss of cyanogen in a single step.[53,54]

The dehydrated compound $Pb[Au(CN)_2]_2$ (**2**) was synthesized in bulk by heating **1** in an oven overnight at 175 °C. The resulting bright yellow powder exhibits a single ν_{CN} peak at 2130 cm^{-1} in the IR and one at 2154 cm^{-1} in the Raman spectrum. In contrast to **1**, no room temperature emission was observed for **2**. Once dehydrated, **2** does not readily rehydrate. Single crystals of **1** degraded upon dehydration, precluding a structural investigation of **2** via single-crystal X-ray diffraction.

(47) Sharpe, A. G. *The Chemistry of Cyano Complexes of the Transition Metals*; Academic Press: London, New York, San Francisco, 1976.
(48) Colacio, E.; Lloret, F.; Kivekäs, R.; Ruiz, J.; Suárez-Varelaa, J.; Sundberg, M. R. *Chem. Commun.* **2002**, 592.
(49) Shi, Y.-J.; Chen, X.-T.; Li, Y.-Z.; Xue, Z.; You, X.-Z. *New J. Chem.* **2002**, *26*, 1711.
(50) Jürgens, B.; Höppe, H. A.; Schnick, W. *Solid State Sci.* **2002**, *4*, 821.
(51) Morsali, A.; Mahjoub, A. R. *Helv. Chim. Acta* **2004**, *87*, 2717.
(52) Dale, S. H.; Elsegood, M. R. J.; Kainth, S. *Acta Crystallogr. C* **2004**, *60*, m76.
(53) Chomic, J.; Cernàk, J. *J. Thermochim. Acta* **1985**, *93*, 93.
(54) Cartraud, P.; Cointot, A.; Renaud, A. J. *J. Chem. Soc., Faraday Trans.* **1981**, *77*, 1561.

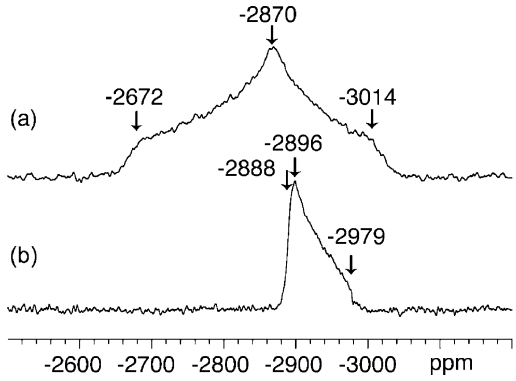

Figure 2. ^{207}Pb nonspinning NMR spectra for (a) **1** and (b) **2** showing the principal components ($\delta_{11} > \delta_{22} > \delta_{33}$) of the chemical shift tensor.

Table 3. NMR Data for **1** and **2** from MAS Spectra (except where noted)

		δ_{iso} (ppm)	Ω (ppm)	κ
^{13}C	**1**	167 ± 1	346 ± 4	>0.95
	2	173 ± 1	353 ± 4	>0.95
^{15}N	**1 (CN(1))**	266 ± 1	480 ± 10	>0.8
	1 (CN(2))	259 ± 1	450 ± 30	>0.7
	2	276 ± 1	n.d.	n.d.
^{207}Pb	**1**	−2850 ± 1	342 ± 5[a]	−0.16 ± 0.07[a]
	2	−2921 ± 1	91 ± 4[a]	0.9 ± 0.1[a]

[a] From nonspinning spectra.

Solid-State NMR. To probe the structure of microcrystalline **2**, multinuclear magic-angle spinning (MAS) and nonspinning NMR of **1** and **2** were performed. ^{13}C and ^{15}N NMR experiments were done on samples prepared with 15% doubly labeled ^{13}C^{15}N to enhance sensitivity. These samples afford the additional advantage that ^{13}C signals are coupled to spin-1/2 ^{15}N, and not the quadrupolar ^{14}N, resulting in higher resolution and less complicated spectra.[55−57]

^{1}H MAS NMR. The ^{1}H MAS NMR spectrum of the hydrated sample **1** possesses signals at 3.7 and 4.9 ppm (Figure S1), corresponding to the H-bonded and non-H-bonded sites present in the crystal. ^{1}H chemical shift systematics for waters H-bonded to N-donor groups are poorly defined and do not permit reliable assignments of these two peaks. Nevertheless, both peaks disappear upon dehydration, thus confirming the loss of water.

^{207}Pb NMR. The hydrated sample, **1**, has a surprisingly small ^{207}Pb chemical shielding span ($\Omega = \delta_{11} - \delta_{33}$) for a nucleus that commonly logs spans up to 3800 ppm (Figure 2a, Table 3).[16] The measured shielding, spanning 342 ppm, is consistent with the relatively regular trigonal prism formed by the N-bound cyanides. The skew ($\kappa = 3(\delta_{22} - \delta_{iso})/\Omega$) of −0.16 differs significantly from axial symmetry (given by $\kappa = +1$ or -1), indicating that all three components of the shielding are markedly different.

After dehydration, the ^{207}Pb MAS NMR spectrum exhibits much broader peaks (FWHM = 840 vs 2000 Hz), indicating a lower degree of crystallinity. There is a relatively small change of 71 ppm in the isotropic chemical shift to lower frequency, which can be understood in terms of the chemical shift components measured from the nonspinning spectra (Figure 2b),

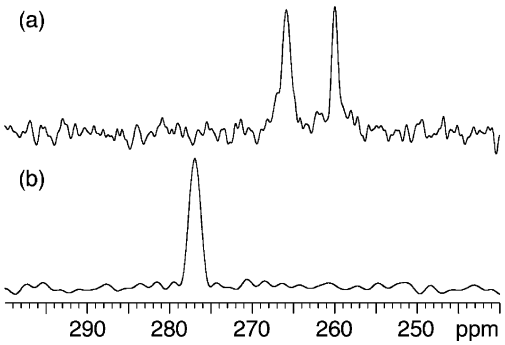

Figure 3. ^{15}N MAS NMR of (a) **1** and (b) **2** spinning at 18 and 17 kHz, respectively.

where it is evident that the Pb center occupies a site of higher symmetry after loss of the structural water. Not only is the span ($\Omega = 91$ ppm) much smaller than that in the hydrated sample, the skew ($\kappa = 0.9 \pm 0.1$) indicates that the lead possesses essentially axial symmetry. Comparing this with the ^{207}Pb NMR spectrum of the hydrated sample, it appears that the most shielded component in **1** ($\delta_{33} = -3014$ ppm) is changed little upon dehydration, whereas the least shielded component ($\delta_{11} = -2672$ ppm) shifts to align with the intermediate component, δ_{22} (vide infra).

^{15}N MAS NMR. Two sites appear in a 1:1 ratio at 259 and 266 ppm in the ^{15}N MAS NMR spectrum (Figure 3a) of isotopically enriched **1**, in agreement with the crystal structure. Since hydrogen bonding has been shown to increase nitrogen shielding,[58,59] the peak at 259 ppm is probably assignable to CN(2), although bonding to one versus two lead atoms may also have an effect on the observed chemical shift. Simulation of the slow-spinning ^{15}N MAS spectra of **1** (not shown) indicates axial symmetry and typical shielding spans for both cyanides (Table 3).[56,60] The expected $^1J(^{13}C,^{15}N)$ of ca. 16 Hz is not observable due to the 130−180 Hz ^{15}N line widths.[61] One-bond *J*-couplings to ^{207}Pb are known to be in the range of 100−300 Hz.[62,63] This would be expected to give rise to low-intensity (10%) satellites; however, no such satellites could be confidently assigned.

The dehydrated sample produces a single ^{15}N peak, slightly higher in frequency than CN(1), indicating a single cyanide site in **2** (Figure 3b).

^{13}C MAS NMR. A single site at 167 ppm is observed in the ^{13}C MAS NMR of isotopically enriched **1** (Figure S2), despite the presence of two crystallographically inequivalent cyanides. This observation indicates that the chemical shielding is dominated by bonding to the gold and is little affected by the presence of water in the second coordination sphere. Upon dehydration, the peak shifts to 174 ppm in **2** (Figure S3), presumably due to the structural adjustment of the cyanides with respect to Pb and Au. Both compounds possess axially sym-

(55) Curtis, R. D.; Ratcliffe, C. I.; Ripmeester, J. A. *J. Chem. Soc., Chem. Commun.* **1992**, 1800.
(56) Kroeker, S.; Wasylishen, R. E.; Hanna, J. V. *J. Am. Chem. Soc.* **1999**, *121*, 1582.
(57) Kroeker, S.; Wasylishen, R. E. *Can. J. Chem.* **1999**, *77*, 1962.
(58) Lorente, P.; Shenderovich, I. G.; Golubev, N. S.; Denisov, G. S.; Buntkowsky, G.; Limbach, H.-H. *Magn. Reson. Chem.* **2001**, *39*, s18.
(59) Shenderovich, I. G.; Buntkowsky, G.; Schreiber, A.; Gedat, E.; Sharif, S.; Albrecht, J.; Golubev, N. S.; Findenegg, G. H.; Limbach, H.-H. *J. Phys. Chem. B* **2003**, *107*, 11924.
(60) Duncan, T. M. *Chemical Shift Tensors*, 2nd ed.; The Farragut Press: Madison, WI, 1997.
(61) Wasylishen, R. E.; Muldrew, D. H.; Friesen, K. J. *J. Magn. Reson.* **1980**, *41*, 341.
(62) Kennedy, J. D.; McFarlane, W.; Pyne, G. S.; Wrackmeyer, B. *J. Organomet. Chem.* **1980**, *195*, 285.
(63) Kennedy, J. D.; McFarlane, W.; Wrackmeyer, B. *Inorg. Chem.* **1976**, *15*, 1299.

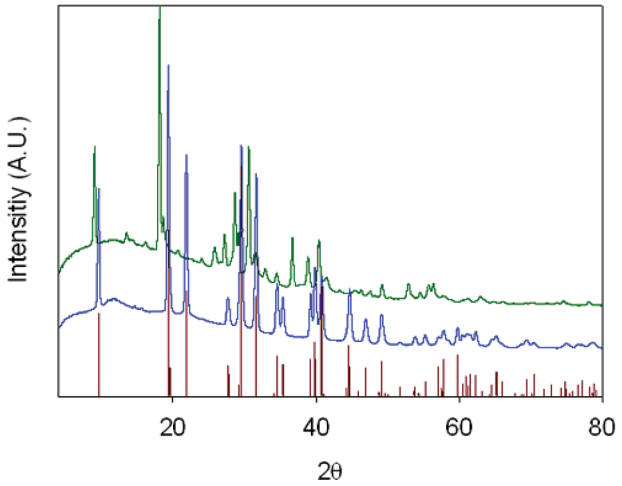

Figure 4. X-ray powder diffractogram of **1** (green), **2** (blue), and simulated peaks for **2** (red).

metric ^{13}C shielding tensors and spans comparable to other diamagnetic metal cyanides (Table 3).[56,60,64]

Structure of $Pb[Au(CN)_2]_2$ (2). The powerful combination of the multinuclear solid-state NMR and X-ray powder diffraction data permits a reasonable proposal for the structure of **2**, despite the lack of single-crystal diffraction data. Indeed, considering the high sensitivity of chemical shifts to local structure, the ^{207}Pb NMR results are crucial in postulating the structure of **2**. For example, ^{207}Pb isotropic chemical shifts of tetrahedral lead in lead oxides range from 1940 to −1300 ppm, whereas eight-coordinated lead sites have shifts of −2000 to −2100.[16] Although the removal of solvents within coordination polymers can yield quite different structures,[28,65−67] the isotropic ^{207}Pb chemical shift of **2** is quite similar to that observed in **1**, implying that the coordination geometry of the Pb(II) is not greatly altered by dehydration. The coordination geometry of the Pb(II) center is also more symmetric than in **1** since the nonspinning ^{207}Pb NMR spectrum of **2** (Figure 2b) indicates essentially axial symmetry ($\kappa = 0.9 \pm 0.1$). In addition, the ^{15}N MAS NMR data show only a single site at 276 ppm (Figure 3b), indicating that all cyanide groups interact equally with the lead. Using the structure of **1** as a reference point, the loss of the H-bond at CN(2) via the removal of the water molecule would result in a CN(2) environment similar, but not identical, to that of CN(1), illustrating that only a small structural rearrangement is necessary to render the two CN groups equivalent. Taking into account the above constraints, the $Pb[Au(CN)_2]_2$ stoichiometry, and also the presence of one down-shifted cyanide in the IR spectrum, the structure of **2** must contain a Pb(II) center surrounded by either eight or four N-bound cyanides. Considering the similar ^{207}Pb chemical shifts in **1** and **2**, relative to the large changes documented for significant changes in the lead coordination number,[16] it may be inferred that a strictly four-coordinate Pb(II) center is highly unlikely in the dehydrated product.

Further structural information can be gleaned from the powder X-ray diffractogram of **2** (Figure 4 and Table S1), which can be indexed to a tetragonal cell having dimensions $a = b =$ 6.40105(13), $c = 18.3662(6)$ Å. Note that starting from **1**, compression of all axes followed by a simple transformation yields the observed cell for **2** ($a_1 \rightarrow a_2$, $2b_1 \rightarrow c_2$, $1/2c_1 \rightarrow b_2$), reinforcing the NMR-based supposition that dehydration of **1** does not radically alter the structure. Thus, using the structure of **1** as a starting point, lead and gold atoms were placed at specific fractional coordinates inside the tetragonal unit cell for **2**, and the resulting crystal symmetry and calculated powder patterns were compared with the experimental data. Several different sets of positions for the gold and lead atoms in **2** were considered, and those which did not conform to the NMR data (which requires axial symmetry about the Pb(II) and equivalent CN groups) were rejected. Of the remaining three models, which differ slightly by either the geometry of the Au layer or the position of the Pb(II) center, only one arrangement of atoms generated a powder pattern comparable in calculated positions and intensities to those observed (Figure 4, Table S2). On this basis, the structure of **2** is proposed to consist of a Pb(II) cation in an eight-coordinate distorted square prismatic geometry (Figure 5a,c), in the space group *I*4/*mcm*. Indeed, this proposed structure can be generated from the known structure of **1** with minimal atomic rearrangement by bonding of the CN(2) nitrogen to the Pb(II) of an adjacent slab (Figure 6b), followed by a minor reorganization of the gold and lead layers. In **2**, the Pb(II)-based prisms stack upon one another, producing a column of prisms, which edge-share to four neighboring columns (Figure 5b). As a result, each gold center forms aurophilic interactions of 3.3 Å to four other gold centers (Figure 5, dashed lines), thereby generating a 2-D array of interlinked gold atoms in the *ab* plane. The aurophilic interactions in **2** are shorter than those observed in **1**. The cyanide units were placed in idealized positions (i.e., using standard, fixed bond lengths for the $Au(CN)_2$ unit) pointing at the Pb(II) in a fashion similar to that observed in **1**

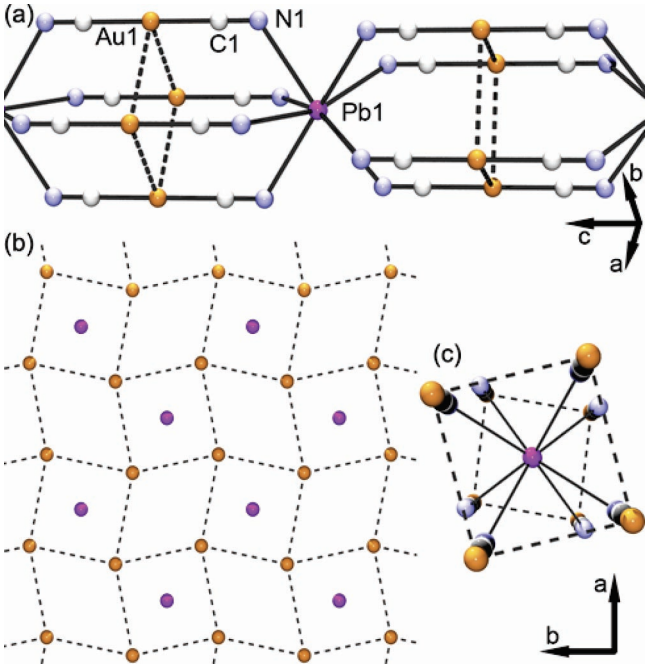

Figure 5. (a) View of **2** showing the column aligned along the *c*-axis, highlighting the Pb(II) coordination sphere and intra-column aurophilic interactions (dashed lines). (b) Single layer of Au(I) atoms in the *ab* plane with Pb(II) atoms in the square channels; dashed lines are aurophilic interactions. (c) Local site geometry of Pb(II) showing the distorted square antiprism.

(64) Wu, G.; Kroeker, S.; Wasylishen, R. E. *Inorg. Chem.* **1995**, *34*, 1595.
(65) Carlucci, L.; Ciani, G.; Proserpio, D. M. *Chem. Commun.* **2004**, 380.
(66) Wang, Z.; Jin, C.-M.; Shao, T.; Li, Y.-Z.; Zhang, K.-L.; Zhang, H.-T.; You, X.-Z. *Inorg. Chem. Commun.* **2002**, *5*, 642.
(67) Cui, Y.; Ngo, H. L.; White, P. S.; Lin, W. *Inorg. Chem.* **2002**, *42*, 652.

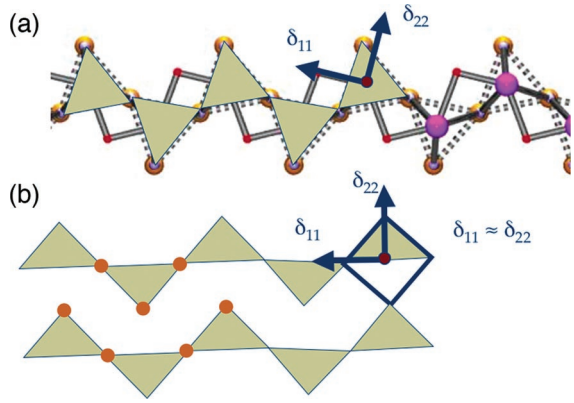

Figure 6. Formation of squares in **2** (b) upon dehydration of **1** (a) via adjacent slabs, including proposed chemical shift tensor orientations with δ_{33} directed out of the plane of the page.

(Figures 1a and 5a), thereby preserving a similar coordination geometry about the Pb(II). It should be noted, however, that since the cyanides do not contribute greatly to the X-ray powder pattern of **2** it is not possible to unambiguously determine whether the cyanide groups bridge two eight-coordinate Pb(II) centers symmetrically (as currently shown) or asymmetrically (as in **1**). In agreement with the NMR interpretation, a four-coordinate lead center would be structurally unreasonable due to the closeness of the gold and lead atoms. Based solely on the placement of the cyanide groups, the Pb−N bond length is approximately 2.8 Å, which is comparable to the 2.595(18), 2.65(2), and 2.87(2) Å in **1**. Interestingly, the structure of **2** has an Anyuiite-type structure (i.e., $AuPb_2$); this mineral family[68] crystallizes in the same space group as **2** (*I*4/*mcm*) with similar fractional coordinates but different unit cells depending on the constituent atoms.

The unique component of the ^{207}Pb shielding tensor (δ_{33}, Figure 2) can only be reasonably directed along the local axis running between the cyanides (Figure 6b), with the nearly degenerate δ_{11} and δ_{22} lying in a plane bisecting the square antiprism (Figure 5). Presumably, the most shielded component also lies along the *b*-axis in **1** since the magnitudes of δ_{33} are very similar and only subtle structural changes are observed upon dehydration of this compound. Because of their structural similarity, it is likely that the least-shielded components in **1** and **2** are confined to the *ac* mirror plane in **1**. In **1**, δ_{11} is probably aligned with the Pb−OH_2 bond, and δ_{22} is not directed along any particular bond (Figure 6a). This interpretation accounts for why the δ_{11} component shifts significantly with the loss of water, while δ_{22} and δ_{33} remain virtually unaltered.

Birefringence. To highlight the potential utility of highly polarizable lead(II)-containing coordination polymers, the birefringence of the plate-shaped single crystals of **1** was measured (Figure 7). Birefringence (Δn), defined as the difference in the refractive index between two directions, is an important optical property often used for common-path profilometry systems,[69] compact-disk readers,[70] image processing, intraocular elements,[71] and many other devices which would be more mechanically cumbersome without birefringent materials.[72−77] Although Δn has been tabulated for many inorganic materials, there are very few such measurements for coordination polymers.[78−80]

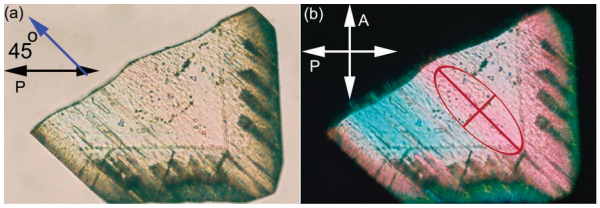

Figure 7. Single crystal of **1** under a polarizing microscope: (a) Single polarizer, P, below the sample. (b) Crystal, in diagonal position, between crossed polarizers, P and A. Directions of the polarizers are indicated by black or white double-headed arrows. The direction of one crystallographic axis (*b* or *c*) is shown by the blue arrow. The red ellipse denotes the *bc* section of the indicatrix.

X-ray analysis reveals that the large faces of the plate-shaped crystals of **1** are oriented perpendicular to the *a*-axis, suggesting that the slowest crystal growth direction is along the *a*-axis. The more rapid crystal growth occurring along the inter-slab axis rather than via slab extension suggests that inter-slab hydrogen bonding and aurophilic interactions may play an important role in the kinetics of crystal growth in this system. In addition, the stereochemical lone pair, whose hemisphere is found oriented close to the *a*-axis, may also inhibit rapid bond formation in that direction. A photograph of the crystal of **1** used to measure the birefringence is shown in Figure 7. The fact that the crystal does not remain dark when rotated between crossed polarizers (Figure 7b) indicates the existence of an optical anisotropy, which is expected for orthorhombic crystals. Between crossed polarizers, the crystal shows complete extinction at specific orientations. The dark streaks observed near the right and bottom crystal edges in Figure 7b can be found in Figure 7a also, and thus they are opaque regions, not part of extinction. The extinction direction in an orthorhombic crystal viewed down the *a*-axis should coincide with the other two crystallographic axes.[81] Thus, the position of the crystallographic axes can be derived from optical observations (Figure 7a, blue arrow); however, it cannot be determined from optical data if the labeled axis is the *b* or *c* direction. With the crystal 45° off of the extinction position, the crystal color appears homogeneous (Figure 7b); the rainbow pattern observed is due to a slight variation in thickness across the platelet. This homogeneity implies that twins and significant internal stresses are absent. This is also confirmed by the fact that the extinction is observed in all parts of the crystal simultaneously; these preliminary observations indicate that the crystal is suitable for a birefringence measurement with confidence.

For the light propagating along the *a*-axis of **1**, a birefringence value of $\Delta n = 7.0 \times 10^{-2}$ at room temperature was measured.

(68) Havinga, E. E.; Damsma, H.; Hokkeling, P. *J. Less-Common Metals* **1972**, *27*, 169.
(69) Chou, C.; Shyu, J.-C.; Huang, Y.-C.; Yuan, C.-K. *Appl. Opt.* **1998**, *37*, 4137.
(70) Kinnstatter, K.; Ojima, M.; Yonezawa, S. *Appl. Opt.* **1990**, *29*, 4408.
(71) Lesso, J. P.; Duncan, A. J.; Sibbett, W.; Padgett, M. J. *Appl. Opt.* **2000**, *39*, 592.
(72) Davis, J. A.; Evans, G. H.; Crabtree, K.; Moreno, I. *Appl. Opt.* **2004**, *43*, 6235.
(73) Kikuta, H.; Iwata, K.; Shimomura, H. *J. Opt. Soc. Am. A* **1992**, *9*, 814.
(74) Sanyal, S.; Ghosh, A. *Appl. Opt.* **2000**, *39*, 2321.
(75) Park, J.-H.; Jung, S.; Choi, H.; Lee, B. *Opt. Express* **2003**, *11*, 1862.
(76) Waagaard, O. H.; Skaar, J. *J. Opt. Soc. Am. A* **2004**, *21*, 1207.
(77) Sanyal, S.; Bandyopadhyay, P.; Ghosh, A. *Opt. Eng.* **1998**, *37*, 592.
(78) Janiak, C.; Scharmann, T. G.; Albrecht, P.; Marlow, F.; Macdonald, R. *J. Am. Chem. Soc.* **1996**, *118*, 6307.
(79) Draper, N. D.; Batchelor, R. J.; Sih, B. C.; Ye, Z.-G.; Leznoff, D. B. *Chem. Mater.* **2003**, *15*, 1612.
(80) Fromm, K. M.; Gueneau, E. D.; Rivera, J.-P.; Bernardinelli, G. *Z. Anorg. Allg. Chem.* **2002**, *628*, 171.
(81) Wahlstrom, E. E. *Optical Crystallography*; John Wiley and Sons: New York, Toronto, 1979.

This is a high value, much larger than the Δn of 0.9×10^{-2} for quartz, 2.7×10^{-2} for Al_2O_3, a material used for birefringent coatings,[82] and indeed larger than most other optical materials.[83] The birefringence of **1** is still below that of commercially important calcite (17.2×10^{-2}), but is higher than the value of 6.38×10^{-2} that we recently obtained for a highly structurally anisotropic Cu(II)/Hg(II) 2-D layered system.[79]

Orthorhombic crystals are optically biaxial, and their indicatrix (i.e., the surface showing the variation of the refractive index, *n*, with the vibration direction of light) is represented by a triaxial ellipsoid having its principal axes parallel to the crystallographic axes.[81] From this, any measured refractive index can be broken down into components along the ellipsoid axes. These three principal refractive indices can be designated as n_a, n_b, and n_c for light propagating along the *a*, *b*, and *c* crystallographic directions, respectively. The above measured birefringence is $\Delta n = \Delta n_{bc} = |n_b - n_c|$; two other values of interest, $\Delta n_{ab} = |n_a - n_b|$ and $\Delta n_{ac} = |n_a - n_c|$, remain unknown. Unfortunately, to determine the remaining birefringence values, and thereby to determine the maximum birefringence and the full indicatrix, crystals with large enough surfaces perpendicular to the *b*- or *c*-axes are required; these are currently unavailable due to difficulties in altering the crystal growth direction.

The measured birefringence of **1** remains practically unchanged upon heating to 340 K and upon cooling actually increases gradually to 7.3×10^{-2} at 200 K, below which no further change occurs, suggesting a "freezing" of the crystal structure. This small temperature dependence of the birefringence indicates the absence of significant changes in the crystal structure in the studied temperature range of 150−340 K since any structural phase transformation would be indicated by an abrupt variation of the birefringence.

The high optical anisotropy can be associated with the 2-D layer crystal structure of **1**. According to the Maxwell relation, at optical frequency, the refractive index is defined by the relative dielectric permittivity (ϵ), $n^2 = \epsilon$.[84] The only contribution to ϵ at this frequency comes from the electronic polarization. The electronic permittivity is proportional in turn to the polarizability of the molecules in the material and to the local electric fields. Local fields that act on the molecule can be very different from the external field applied to the crystal, due to interactions with neighboring molecules. The electronic polarizability of covalent bonds in molecules is usually strongly anisotropic and, if the directions of the bonds are ordered in the crystal structure, this leads to the anisotropy of the permittivity (i.e., to birefringence). This is best exemplified by the coordination sphere around the lead, which orients all of the $[Au(CN)_2]^-$ moieties in only one direction (Figure 1); this indicates that the polarizable lead(II) cation also plays a very significant structural role in determining the observed optical properties. Another possible reason for a large Δn is the anisotropy of local fields.[85] However, due to the large number of atoms and differently directed bonds in the structure of **1**, the anisotropy of total polarizability and the anisotropy of the local fields (i.e., the main sources of birefringence) cannot be even qualitatively estimated.

Conclusion

The lead(II) cyanoaurate coordination polymer, $Pb(H_2O)[Au(CN)_2]_2$, and its dehydrated analogue have been prepared and structurally and optically characterized. This work illustrates the power of solid-state NMR techniques for gaining structural information about coordination polymers. Given the challenges of obtaining single crystals of coordination polymers, this multinuclear magnetic resonance approach deserves renewed attention particularly for cyanometalate systems, which can be readily $^{13}C^{15}N$-labeled for convenient spectral acquisition. $Pb(H_2O)[Au(CN)_2]_2$ was found to have a high optical birefringence with a $\Delta n = 7.0 \times 10^{-2}$ at 300 K, attributable to the structural anisotropy. Judicious modification of the modular building blocks in **1** with other polarizable groups could potentially generate materials with even higher birefringence.

Acknowledgment. Financial support from NSERC of Canada and Natural Resources Canada (M.J.K.) is gratefully acknowledged. The Varian Inova 600 and Thermo Nicolet Nexus 670 FT-Raman spectrometers (University of Manitoba) are supported by the Canada Foundation for Innovation and the Province of Manitoba.

Supporting Information Available: X-ray crystallographic file (CIF) for $Pb(H_2O)[Au(CN)_2]_2$ **1**. Powder X-ray data for **2** and additional solid-state NMR spectra. This material is available free of charge via the Internet at http://pubs.acs.org.

JA0566634

(82) Hodgkinson, I. J.; Wu, Q. H. *Birefringent Thin Films and Polarizing Elements*; World Scientific Publishing Co. Pte. Ltd.: River Edge, 1997.
(83) Veber, M. J. *Handbook of Optical Materials*; CRC Press: Boca Raton, FL, 2003.
(84) Chelkowski, A. *Dielectric Physics*; Elsevier Scientific Pub. Co: Amsterdam, New York, 1980.
(85) Newnham, R. E. *Structure−Property Relations*; Springer-Verlag: New York, Heidelberg, Berlin, 1975.